





China Space Station Telescope and Variable Star Studies

Xiaodian Chen^{1,2,3} , Shu Wang^{1,2,3} , Licai Deng^{1,2,3},
Richard de Grijs^{4,5}, Xiaoyue Zhou¹, Xiaohan Chen¹ and
Jianxing Zhang¹

¹CAS Key Laboratory of Optical Astronomy, National Astronomical Observatories, Chinese Academy of Sciences, Beijing, China
email: chenxiaodian@nao.cas.cn

²School of Astronomy and Space Science, University of the Chinese Academy of Sciences, Beijing, China

³Department of Astronomy, China West Normal University, Nanchong 637009, China

⁴School of Mathematical and Physical Sciences, Macquarie University, Balaclava Road, Sydney, NSW 2109, Australia

⁵Astrophysics and Space Technologies Research Centre, Macquarie University, Balaclava Road, Sydney, NSW 2109, Australia

Abstract. In the last five years, the number of periodic variable stars has increased by two million. We used the ZTF DR2 data to find and build a catalog that includes 780,000 periodic variable stars. These periodic variable stars were classified into 11 types, which greatly complemented the variable stars in Galactic disk. Based on the latest ZTF DR16 data, we found 2 million variable candidates. We trained a machine learner to classify variable stars, and the learner had a prediction accuracy of 94%. Using millions of variable stars, we carried out studies to optimize the period–luminosity relations and the Galactic structure and the extinction law. With the future China Space Station Telescope, millions of variable stars in the Local Group will be discovered. They help to study the structure of our Local Group and also to cross-check the distance ladders based on different variable stars.

Keywords. Periodic variable stars, Cepheid variable stars, RR Lyrae variable stars, Galaxy structure, Distance indicators

1. Introduction

Variable stars have been studied for hundreds of years, and the number of known variable stars has increased rapidly in the last decade. Some variable stars undergo periodic changes in their luminosity and are called periodic variable stars. There are three main categories of periodic variable stars: pulsating stars, eclipsing binaries, and rotational variable stars. Periodic variable stars can be important distance tracers when they satisfy a simple linear relation between period and luminosity, i.e., the period–luminosity (PL) relation. A large number of periodic variable stars can help to optimize the distance estimates of the galaxies, to understand the three-dimensional (3D) structure of the Milky Way and our Local Group, and to optimize the Hubble constant.

Efficient variable star searches through large fields of view began in the 1990s. The Massive Compact Halo Object survey (Alcock et al. 1993) found 20,000 variable stars in the Large Magellanic Cloud (LMC). The Optical Gravitational Lensing Experiment

(OGLE, Udalski *et al.* 1992, 2015) has discovered about one million variable stars in nearly 30 years of observations. For the first 20 years, OGLE focused on the LMC and Small Magellanic Cloud (SMC), and in the last decade it has shifted to searching for variable stars in the Galactic bulge and the southern disk. The first all-sky variable star survey was performed by the All-Sky Automated Survey (ASAS, Pojmanski *et al.* 2005), which found nearly 20,000 periodic variable stars. A deeper search for all-sky variable stars was the Catalina survey (Drake *et al.* 2014, 2017), which discovered about 100,000 periodic variable stars. The RR Lyrae stars in this catalog were very useful for studying the Galactic halo and streams. The VISTA Variables in the Vía Láctea (VVV, Minniti *et al.* 2010) survey was an infrared survey that looked for variable stars in the inner disk of the Milky Way. A large number of variable star catalogs were published in 2018. In addition to OGLE, there were the Wide-field Infrared Survey Explorer (WISE) catalog of periodic variable stars (Chen *et al.* 2018), the All-Sky Automated Survey for Supernovae (ASAS-SN, Jayasinghe *et al.* 2018), the Asteroid Terrestrial-impact Last Alert System (ATLAS, Heinze *et al.* 2018), and the variable catalog of Gaia DR2 (Mowlavi *et al.* 2018; Clementini *et al.* 2019). These variable catalogs made up for the many variables missing from the Galactic disk, leading to the presentation of a 3D intuitive map of the disk (Chen *et al.* 2019; Skowron *et al.* 2019).

Subsequently, the Zwicky Transient Facility (ZTF) catalog of periodic variable stars (Chen *et al.* 2020) was the largest variable star catalog in the northern sky, including 780,000 periodic variable stars. Gaia DR3 released the largest variable star catalog to date (Rimoldini *et al.* 2023), including three million periodic variable stars. Future telescopes, including the China Space Station Telescope (CSST) and the Vera C. Rubin Observatory Legacy Survey of Space and Time (LSST), will provide opportunities to discover more extragalactic variable stars. In this paper, we introduce the ZTF catalog of periodic variable stars in Section 2. Section 3 describes our update of this catalog using the latest ZTF data. We discuss our recent studies using variable stars in Section 4. Section 5 is a summary.

2. Periodic variable stars in ZTF DR2

ZTF is a 48-inch Samuel Oschin telescope operating at the Palomar Observatory (Bellm *et al.* 2019). It has a large field of view (47 square degrees) to capture transient objects. Its public survey program began in March 2018. The survey is scheduled to observe the majority of the northern sky every three days and to observe the Galactic northern disk ($|l| < 7^\circ$) once a day. The ZTF observations have a fixed exposure time of 30 seconds and its corresponding limiting magnitudes in the g, r bands are about 20.5 mag. The main science of the ZTF is to search for transient objects, including supernovae, tidal disruption events, and near Earth asteroids or comets.

We used the ZTF DR2 data to search for periodic variable stars (Chen *et al.* 2020). The time span of the photometric data is 470 days, which is sufficient for a more accurate determination of the period up to ~ 200 days. The Lomb-Scargle periodogram (Lomb 1976; Scargle 1982) was used to analyze the light curves, and we accepted periodic variable stars when the false-alarm probability of the peaks of the periodogram is less than 0.001. Once excluding aliased periods, such as $P = 0.5, 1, 2, \dots$, the most dominant peak on the periodogram is considered to be the period of one candidate. We then used the period to

calculate the phases and adopted a Fourier function $f = a_0 + \sum_{i=1}^4 a_i \cos(2\pi it/P + \phi_i)$ to fit the phase-folded light curve. By using the coefficient of determination of the fit R^2 , we excluded candidates with poorly fitted light curves.

Table 1. All and new periodic variable stars in ZTF DR2.

Type	Total	New (fraction)
Cep-I	1262	565 (44.8%)
Cep-II	358	154 (43.0%)
RRab	32,518	3034 (9.3%)
RRc	13,875	2178 (15.7%)
EW	36,9707	306,375 (82.9%)
EA	49,943	40,201 (80.5%)
δ Scuti	16,709	15,396 (92.1%)
Mira	11,879	4,997 (42.1%)
SR	119,261	97,737 (82.0%)
RS CVn	81,393	70,957 (87.2%)
BY Dra	84,697	80,108 (94.6%)
Total number	781,602	621,702 (79.5%)

We obtained a sample of 780,000 periodic variable stars, 74% of which are located in the Galactic disk, where previous surveys were very incomplete. Compared to the previous variable star catalogs, 80% of periodic variable stars in our sample are newly discovered. We classified these variable stars using the Density-Based Spatial Clustering of Applications with Noise (DBSCAN) method, with parameters including period, phase difference ϕ_{21} , amplitude, amplitude ratio R_{21} , luminosity, and R^2 . The final periodic variable stars were classified into 11 types, including classical Cepheids, type-II Cepheids, fundamental RR Lyrae (RRab) stars, first-overtone RR Lyrae (RRc) stars, δ Scuti stars, EW-type eclipsing binaries, EA-type eclipsing binaries, Miras, semi-regular (SR) variable stars, RS CVn variables and BY Dra variables (see Table 1). Pulsating variable stars and eclipsing binaries with large amplitudes were clearly distinguished using period and light curve parameters (phase difference, amplitude, and amplitude ratio). For pulsating variables with smaller amplitudes and rotational variable stars, the luminosity is required to help their classification. The luminosity was calculated using the Gaia parallax.

3. More variable stars in ZTF DR16

What is more for ZTF variable stars? The currently available catalog is ZTF DR16, which has an increased time span from 470 to 1750 days compared to DR2. The number of epochs in r band has increased from 150 to 350. In our preliminary analysis, the number of periodic variable stars will increase to 2 million. We also plan to add the classification of double-mode variable stars and to add the parameters of eclipsing binaries, such as the depth and duration of the eclipse.

By analyzing the periodogram of each object in ZTF DR16, we identified 2 million periodic variable candidates. As for classification, we tried different machine learning methods and found that the bagged tree method was most suitable. To train the classification learner, we used 0.6 million variable stars from the ZTF DR2 catalog, and the classification accuracy is 93.9% by five-fold cross-validation. The confusion matrix is shown in Fig. 1. The positive prediction ratios are above 90% for all variable stars except the type-II Cepheids and rotational variable stars. It should be noted that if the subtype classification is not considered, the accuracy will be about 99%. As for the feature importance in the classification, the most important feature is the period P , followed by the amplitude ratio R_{21} , the phase difference ϕ_{21} and the amplitude (Amp.). The parallax ϖ and absolute magnitude $M_{W_{gr}}$ are also helpful to improve the accuracy of classification. The maximum value of the power spectral density (PSD), the fit parameters R^2 and root mean square error (RMSE), and the amplitude ratio R_{31} are not very important (see Fig. 2).

Compared to ZTF DR2, there is an increase of 1.2 million periodic variable stars based on ZTF DR16. The new sample includes ~ 600 classical Cepheids, $\sim 100,000$ RR Lyrae

True Class	BYDra	13191	7	3		269	1352		69	134	1683	2
	CEP	12	1116	25		2	20		16	1	35	7
	CEPII	9	56	202			45	4	4		39	10
	DSCT				14955	2	540			3	293	
	EA	126			1	48855	4162	1		1	381	75
	EW	952	13	12	316	4216	372317	4	13	450	5176	571
	Mira							8051				406
	RR	39	2	2		2	35		34937	168	66	
	RRc	35	3		4	2	1016		83	13545	102	
	RSCVN	1159	25	14	521	482	10304		111	270	33869	66
	SR	1	3	3		16	216	297	1		122	22783
			BYDra	CEP	CEPII	DSCT	EA	EW	Mira	RR	RRc	RSCVN
		Predicted Class										

Figure 1. The confusion matrix of our trained learner based on 0.6 million variable stars from the ZTF DR2 catalog.

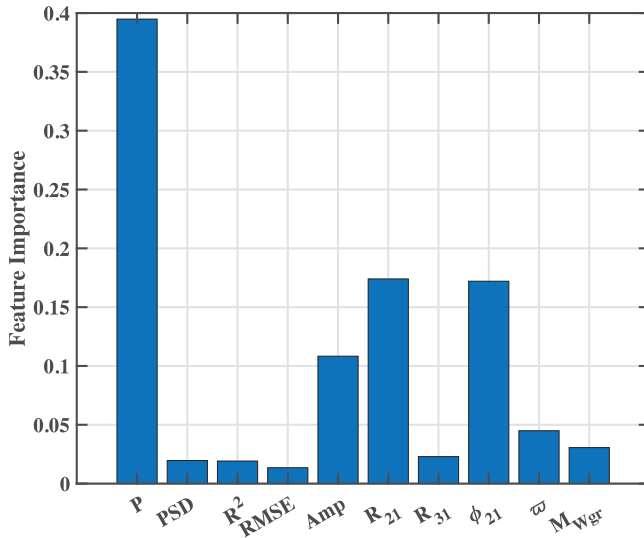


Figure 2. The importance of ten parameters in the classification of periodic variable stars.

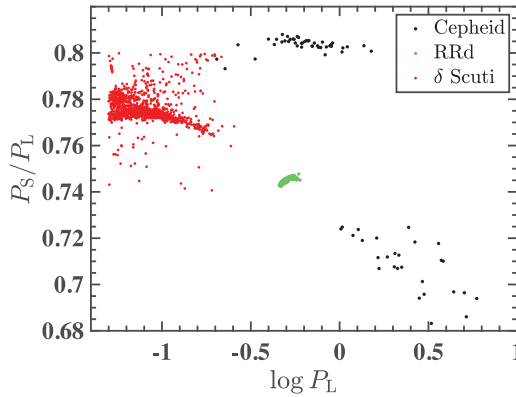


Figure 3. Period–period ratio diagram (Petersen diagram) for δ Scuti stars (red), RR Lyrae stars (green), and classical Cepheids (black). Short and long periods are determined based on ZTF photometry.

stars and $\sim 800,000$ eclipsing binaries. When compared to Gaia DR3, we found that 73% of the sample was in the Gaia variable catalog. This means that Gaia will find the other 20 – 30% new periodic variable stars in future data releases. The agreement rate for the classification of these two catalogs is close to 99%. For Cepheids, the agreement rate of the classification is slightly lower, about 85%, but the classification of Cepheids can be optimized by visually checking each light curve. For the other variable stars, we planned to check some light curves and thus found some criteria to help the classification.

ZTF DR16 is very suitable for identifying double-mode variable stars. Currently we have classified double-mode variable stars in the DR2 catalog (see Fig. 3). The double-mode variable stars are a very important tracer for metallicity and distance (Chen et al. 2023). In the future, when more dynamical mass measurements are determined to optimize the models, they will become accurate mass tracers. In ZTF DR16, we will find more than 5000 double-mode variable stars.

4. Variable star studies

With millions of periodic variable stars, the PL relation or period–metallicity–luminosity relation of periodic variable stars can be optimized. Moreover, based on more distance tracers, it can help to investigate the Milky Way structure and the extinction law.

We presented a 3D intuitive map of the Milky Way using 1339 high-confidence classical Cepheids selected from the variable star catalogs of WISE, ASAS-SN and ATLAS (Chen et al. 2019). We found that the Galactic disk is warped and can be represented by a linear model of $Z_w = 0.148 \times (R - 9.26) \sin(\phi - 17.4^\circ)$ kpc. Here, Z_w , R and ϕ are the height, onset radius and the angle of the line of nodes (LONs) of the warp. Based on structure and kinematics, we found that the precession of the warp, i.e., the warp LONs are changeable for different galactocentric radii. Recently, based on the proper motion and radial velocity data of ~ 700 classical Cepheids from the Gaia DR3, we analyzed the Milky Way warp from 3D kinematics and determined a warp precession rate of $\omega = 4.4 \pm 2.9 \text{ km s}^{-1} \text{ kpc}^{-1}$. Our values are between Poggio et al. (2020) and Chrobáková & López-Corredoira (2021) and support a low warp precession rate.

Open cluster Cepheids (OCCs) are suitable objects for establishing PL relations and period–age relations for classical Cepheids. We performed a census of Galactic OCCs using Gaia early DR3 parallaxes and proper motions, and obtained a total of 33 OCCs,

13 of which are newly discovered (Zhou & Chen 2021). Based on them, we established PL relations of classical Cepheids in Gaia and WISE bands as $M_{G, BP, RP} = -3.32 \log P + (-2.718 \pm 0.049)$ and $M_{W1} = -(3.274 \pm 0.090) \log P + (-2.567 \pm 0.080)$, respectively, which are consistent with the literature (Wang *et al.* 2018; Ripepi *et al.* 2019). Based on the cluster ages, we obtained the period–age (PA) relation for fundamental Cepheids as $\log t = -(0.638 \pm 0.063) \log P + (8.569 \pm 0.057)$. The overtone Cepheid is 0.2 dex younger than the fundamental Cepheid at a given period. The error in the PA relation is 17%, and our PA relation is consistent with the model of Anderson *et al.* (2016), and 0.3 dex older than the model of Bono *et al.* (2005). It should be noted that the PA relation is better constrained at the older end, but not at the younger end. It is important to search for OCCs with longer periods in younger cluster in the future.

Based on a larger sample, the infrared PL relations of LPVs can be optimized. How the metallicity affects the zero point of the PL relation is still very uncertain. We used the Gaia DR3 LPVs (Lebzelter *et al.* 2023) and classified them into red giant branch stars, asymptotic giant branch (AGB) stars and red supergiant stars based on the color and absolute magnitude. The majority of LPVs are AGB stars, and we focused on them and classified them as oxygen-rich (O-rich) and carbon-rich (C-rich) AGB stars based on the color. Combining the WISE photometric data, we determined the PL relations for O-rich and C-rich AGB stars in the Milky Way, LMC and SMC, respectively. The PL relations of AGB stars include several sequences, C (fundamental mode), C' (first-overtone mode), B (second-overtone mode) and D (long secondary period) sequences (Wood *et al.* 1999). Among them, the C sequence is often used for distance measurements. We found that for C-rich AGB stars with different amplitudes, the W_2 -band PL relations are different. Large amplitude C-rich AGB stars have a steeper PL relation, which can be explained by the amount of circumstellar dust. During the pulsation, they expand more and produced more circumstellar dust, which leads to a brightening in the mid-infrared magnitudes. Therefore, the near-infrared bands are more suitable for distance measurements using C-rich AGB stars than the mid-infrared bands. We also investigated the metallicity effect based on about 400 AGBs in LMC and SMC with Apache Point Observatory Galactic Evolution Experiment (APOGEE, Majewski *et al.* 2017) DR17 metallicities (see Fig. 4). The PL relation of C-rich AGB stars is not affected by the metallicity, while the PL relation zero point of O-rich AGB stars becomes brighter with the increasing metallicity. The metallicity effect of O-rich AGB stars is similar to that of the classical Cepheids. The coefficients of the metallicity effect are between $\beta = -0.7$ mag/dex and $\beta = -0.3$ mag/dex for C and C' sequences of the LMC and SMC. This suggests that the metallicity effect should be considered when measuring distances with O-rich AGB stars or O-rich Miras.

The PL relations of variable stars can be used to determine the extinction laws. We studied the classical Cepheids in different regions of LMC and SMC with different extinctions (Wang & Chen 2023). The differences in the apparent magnitudes or colors of classical Cepheids at the same period reflect the extinction and color excesses. Based on them, we estimated the extinction coefficients of the LMC and SMC as $A_{G_{RP}}/E(G_{BP} - G_{RP}) = 1.589 \pm 0.014$ and $A_{G_{RP}}/E(G_{BP} - G_{RP}) = 1.412 \pm 0.041$. Based on the multi-band photometry and APOGEE spectral parameters of red supergiants, the multi-band color excess ratios $\frac{E(\lambda - G_{RP})}{E(G_{BP} - G_{RP})}$ were determined. Combining the extinction coefficients and the color excess ratios, we determined the extinction laws of the LMC and SMC from optical to near-infrared, where the total-to-selective extinction ratio R_V is 3.40 ± 0.07 and 2.53 ± 0.10 , respectively. The extinction law of the Milky Way (Wang & Chen 2019) is between those of the LMC and SMC, and we updated the classical extinction laws (Cardelli *et al.* 1989) by combining our results on these three galaxies. The current extinction laws specific to different environments can be represented by analytical equations (see Equ. 1-5) on wavelength λ . Compared with the classical extinction

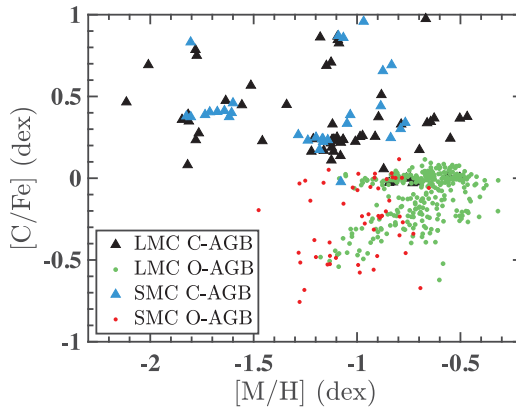


Figure 4. Metallicity and Carbon abundance distributions of C-rich and O-rich AGB stars in LMC and SMC. C-rich AGB stars have a high Carbon abundance. O-rich AGB stars in LMC have a higher metallicity than those in SMC.

law, our results are significantly optimized at wavelengths longer than 600 nm.

$$A_\lambda/A_V = A + B/R_V \quad ; \quad (1)$$

Optical: $0.3 \mu\text{m} < \lambda < 1.0 \mu\text{m}$ and $Y = 1/\lambda(\mu\text{m}) - 1.82$,

$$\begin{aligned} A = & 1.0 + 0.7499Y - 0.1086Y^2 - 0.08909Y^3 \\ & + 0.02905Y^4 + 0.01069Y^5 \\ & + 0.001707Y^6 - 0.001002Y^7 \quad ; \end{aligned} \quad (2)$$

$$\begin{aligned} B = & (1.41338Y + 2.28305Y^2 + 1.07233Y^3 \\ & - 5.38434Y^4 - 0.62251Y^5 + 5.30260Y^6 \\ & - 2.09002Y^7) \times (1 - R_V/3.1) \quad . \end{aligned} \quad (3)$$

Near-IR: $1.0 \mu\text{m} \leq \lambda < 3.33 \mu\text{m}$,

$$A = (0.3722 \pm 0.0026)\lambda^{-2.07 \pm 0.03} \quad ; \quad (4)$$

$$B = (-0.5182 \pm 0.0067)\lambda^{-2.07 \pm 0.03} \times (1 - R_V/3.1) \quad . \quad (5)$$

5. Searching for variable stars with CSST

The CSST is a 2-meter space telescope in the same orbit as the China Manned Space Station and is scheduled to be launched late in 2024. The telescope is equipped with five instruments, of which the Survey Camera is the primary instrument. The Survey Camera has a field of view of 1.1 square degrees and a spatial resolution of 0.15 arc seconds. It will occupy 70% of the CSST’s operating time to observe a 17,500 square degree area of the sky in 10 bands. These bands include seven photometric bands (*NUV, u, g, r, i, z, y*) and three slitless spectra bands covering wavelengths from 255 nm to 1000 nm. The exposure time of the survey is 150 seconds, corresponding to a 5σ limit magnitude of $g = 26.2$ mag. The main science goals of the CSST involve galaxies and cosmology, so the survey avoids the Galactic disk.

The CSST main survey will only observe an object twice in each band, which is not enough for discovering periodic variable stars. We have proposed to perform 20-50 observations of nearby galaxies and dwarf galaxies in the *g* and *r* bands during the test phase. Based on these data, it will be possible to detect periodic variable stars from bright to

faint in LMC and SMC, including Cepheids, RR Lyrae stars, eclipsing binaries, rotational variable stars, δ Scuti, Miras and SRs. We will also search for Cepheids and RR Lyrae stars in ~ 100 nearby galaxies and dwarf galaxies. We expect to find 1 to 2 million periodic variable stars that will be very helpful to check the consistency of different distance tracers. Based on different distance tracers, we plan to obtain high-precision ($\sigma < 2\%$) distances for dwarf galaxies or galaxies and to present a 3D intuitive map of the Local Group.

6. Summary

In order to search for variable stars more sensitively in the northern sky, we used ZTF DR2 light curves to find and build a catalog including 780,000 periodic variable stars. Based on parameters such as period, light curve parameters, and luminosity, these periodic variable stars were classified into 11 types. 74% of these variable stars are located in the Galactic disk, and 80% are new discovered. This catalog provides an opportunity to study periodic variable stars by a large sample size. Based on the latest ZTF DR16 data, we found 2 million variable star candidates. We trained a learner for variable star classification using the sample of ZTF periodic variable star catalog, and the prediction accuracy of the learner is 94%. By comparing with Gaia DR3, we found an agreement rate of 99% for the classification. Gaia can discover another 20%-30% of variable stars in future data releases.

Millions of new periodic variable stars help to study PL relations, Galactic structure and extinction laws. We used more than one thousand classical Cepheids to establish the 3D map of the Milky Way disk and found the warp is in precession. Based on kinematic parameters of classical Cepheids, we obtained a low precession rate of the warp $\omega = 4.4 \pm 2.9 \text{ km s}^{-1} \text{ kpc}^{-1}$. We performed a census of OCCs and obtained 33 OCCs, based on which we determined a PA relation as $\log t = -(0.638 \pm 0.063) \log P + (8.569 \pm 0.057)$. We obtained the extinction laws of the LMC and SMC using classical Cepheids and red supergiants. Combining the Galactic extinction laws, we updated the analytic equations of the extinction laws for different environments R_V . We investigated the PL relations of LPVs and found that the mid-infrared PL relations of C-rich AGB stars are affected by circumstellar dust. For O-rich AGB stars, their PL relation is affected by the metallicity, and the metallicity effect needs to be considered in the distance measurement.

With future CSST, million of variable stars in the Local Group will be found. They help to study the structure of our Local Group, as well as to cross-check the distance ladders of different variable stars.

Acknowledgments: We acknowledge support from the National Natural Science Foundation of China through grants 12173047, 12003046, 12233007, 12133002 and 11903045.

References

- Alcock, C., Akerlof, C.W., Allsman, R.A., et al. 1993, *Nature*, 365, 621
 Anderson, R.I., Saio, H., Ekström, S., Georgy, C., & Meynet, G. 2016, *A&A*, 591, A8
 Bellm, E.C., Kulkarni, S.R., Graham, M.J., et al. 2019, *PASP*, 131, 018002
 Bono, G., Marconi, M., Cassisi, S., et al. 2005, *ApJ*, 621, 966
 Cardelli, J.A., Clayton, G.C., & Mathis, J.S.: 1989, *ApJ*, 345, 245
 Chen, X., Wang, S., Deng, L., et al. 2018, *ApJS*, 237, 28
 Chen, X., Wang, S., Deng, L., et al. 2019, *NatAs*, 3, 320
 Chen, X., Wang, S., Deng, L., et al. 2020, *ApJS*, 249, 18
 Chen, X., Zhang, J., Wang, S., & Deng, L. 2023, *NatAs*, arXiv:2306.10708
 Chrobáková Ž., López-Corredoira M. 2021, *ApJ*, 912, 130
 Clementini, G., Ripepi, V., Molinaro, R., et al. 2019, *A&A*, 622, A60

- Drake, A.J., Graham, M.J., Djorgovski, S.G., et al. 2014, *ApJS*, 213, 9
- Drake, A.J., Djorgovski, S.G., Catelan, M., et al. 2017, *MNRAS*, 469, 3688
- Heinze, A.N., Tonry, J.L., Denneau, L., et al. 2018, *ApJ*, 156, 241
- Jayasinghe, T., Kochanek, C.S., Stanek, K.Z., et al. 2018, *MNRAS*, 477, 3145
- Lebzelter, T., Mowlavi, N., Lecoœur-Taïbi, I., et al. 2023, *A&A*, 674, A15
- Lomb, N.R. 1976, *Ap&SS*, 39, 447
- Majewski, S.R., Schiavon, R.P., Frinchaboy, P.M., et al. 2017, *ApJ*, 154, 94
- Minniti, D., Lucas, P.W., Emerson, J.P., et al. 2010, *NewA*, 15, 433.
- Mowlavi, N., Lecoœur-Taïbi, I., Lebzelter, T., et al. 2018, *A&A*, 618, A58
- Poggio E., Drimmel R., Andrae R., et al. 2020, *NatAs*, 4, 590
- Pojmanski, G., Pilecki, B., and Szczygiel, D. 2005, *AcA*, 55, 275
- Rimoldini, L., Holl, B., Gavras, P., et al. 2023, *A&A*, 674, A14
- Ripepi, V., Molinaro, R., Musella, I., et al. 2019, *A&A*, 625, A14
- Scargle, J.D. 1982, *ApJ*, 263, 835
- Skowron, D. M., Skowron, J., Mróz, P., et al. 2019, *Science*, 365, 478
- Wang, S., Chen, X., de Grijs, R., et al. 2018, *ApJ*, 852, 78
- Wang, S., & Chen, X. 2019, *ApJ*, 877, 116
- Wang, S., & Chen, X. 2023, *ApJ*, 946, 43
- Wood P. R., Alcock C., Allsman R. A., et al., 1999, *IAUS*, 191, 151
- Udalski, A., Szymanski, M., Kaluzny, J., et al. 1992, *AcA*, 42, 253
- Udalski, A., Szymański, M.K., and Szymański, G. 2015, *AcA*, 65, 1
- Zhou, X. & Chen, X. 2021, *MNRAS*, 504, 4768

7. Discussion

Question (Whitelock): I may have missed it, but where did your metallicities come from for the AGB stars?

Answer: The metallicities are from APOGEE.

Question (Abdollahi): Which algorithm (model) do you use to classify these variable stars (the machine learning method)?

Answer: Random forest. This method gives an initial classification of variable stars, and then we optimized the classification for different types of variable stars by manually checking the light curve or establishing parameter-based criteria.

Question (Hajdu): Do you have an idea about the saturation limits of the CSST during its normal operation?

Answer: No. I'm not the person who knows. They might test the scanning mode to observe bright stars.